

RESEARCH ARTICLE

Design, synthesis, cytotoxic evaluation, and QSAR study of some 6H-indolo[2,3-b]quinoxaline derivatives

N. S. Hari Narayana Moorthy, C. Karthikeyan, and Piyush Trivedi

School of Pharmaceutical Sciences, Rajiv Gandhi Technical University, Gandhi Nagar, Bhopal, India

Abstract

In the pathway of anticancer drug development, we designed and synthesized some 6H-indolo[2,3-b]quinoxaline derivatives (which act as DNA intercalators) by structural modification. The structure of the 6H-indolo[2,3-b]quinoxaline derivatives was confirmed by IR, NMR, Mass and elemental analysis. The compounds (IDQ-5, IDQ-10, IDQ-11, IDQ-13, and IDQ-14) exhibited significant *in vitro* activity against a human leukemia (HL-60) cell line. The QSAR derived for modeling the cytotoxic activity of 6H-indolo[2,3-b]quinoxaline derivatives suggests that candidate structures for increased cytotoxic potency should incorporate cyclic substituents or substituents with primary carbon atoms.

Keywords: 6H-indolo[2,3-b]quinoxaline; cytotoxicity; HL-60; QSAR; *in silico*

Introduction

Cancer is the second most common cause of death in the world, after heart disease. The World Health Organization (WHO) estimated that by 2020, 20 million new cases of cancer will be diagnosed each year, and 75% of these will occur in nations that between them have only 5% of resources. At present, it is estimated that ~1 million new cancer cases per annum will be recorded. The effectiveness of cancer chemotherapy is mostly limited by the lack of selectivity of anticancer agents and the occurrence of intrinsic or acquired resistance, leading to significant side effects and sometimes failure of treatments¹⁻⁴.

Anticancer drug toxicities include nausea, vomiting, alopecia, bone marrow depression, and many more. In the course of anticancer drug development, it is necessary to develop extremely potent and less toxic compounds. The discovery of new compounds with antitumoral activity has become one of the goals of medicinal chemistry^{6,7}. Drug design is an effort to develop drugs on a rational basis. The design of drugs reduces trial and error factors as well as the cost of screening large numbers of molecules. Analog design is most fruitful in the study of pharmacologically active

molecules that are structurally specific. Their biological activity depends on the nature and details of their chemical structure.

A literature survey showed that over the past 10 years, the search for new cytotoxic agents has mainly followed classical approaches: structural modifications to conventional molecules, new natural products and modifications of them, potential synthetic compounds and chemical conjugates. Research in this area has not been without benefits, however, for it has produced much information on the synthesis and antitumoral properties of hundreds of compounds, which have been tested on diverse tumoral cell lines⁸⁻¹². In the present work, it was attempted to design and synthesize some compounds with the 6H-indolo[2,3-b]quinoxaline nucleus as polycyclic pharmacophore and evaluate their cytotoxic activity.

6H-Indolo-[2,3-b]quinoxaline is an analog of the cytotoxic agent ellipticine. The first 6H-indolo-[2,3-b]quinoxaline derivatives were prepared in 1895 by the condensation of 1,2-diaminobenzene with isatin; these compounds have the combined structural features of indoles and quinoxalines¹³. In recent years, 6H-indolo[2,3-b]quinoxaline derivatives

Address for Correspondence: Dr N. S. Hari Narayana Moorthy, MPharm, PhD, Rajiv Gandhi Technical University, School of Pharmaceutical Sciences, Airport Bypass Road, Gandhi Nagar, Bhopal, 462036 India. E-mail: nshnm@yahoo.co.in

(Received 26 April 2009; revised 10 July 2009; accepted 17 July 2009)

ISSN 1475-6366 print/ISSN 1475-6374 online © 2010 Informa UK Ltd
DOI: 10.3109/14756360903190747

<http://www.informahealthcare.com/enz>

RIGHTS LINK
Copyright Clearance Center

have received much attention, due to their variety of pharmacological activities such as anticancer activity and antiviral activity against herpes simplex virus type 1 (HSV-1), cytomegalovirus (CMV), varicella-zoster virus (VZV), etc.¹⁴⁻¹⁶. It has been reported that the mechanism of the antiviral and cytotoxic action of the derivatives involves intercalation into the DNA helix and, thus, disturbance of the processes that are vital for DNA replication^{14,17}. Hence, the indolo[2,3-*b*]quinoxaline nucleus was considered as a template for the design and development of DNA intercalating agents with cytotoxic activities in this study.

Chemistry

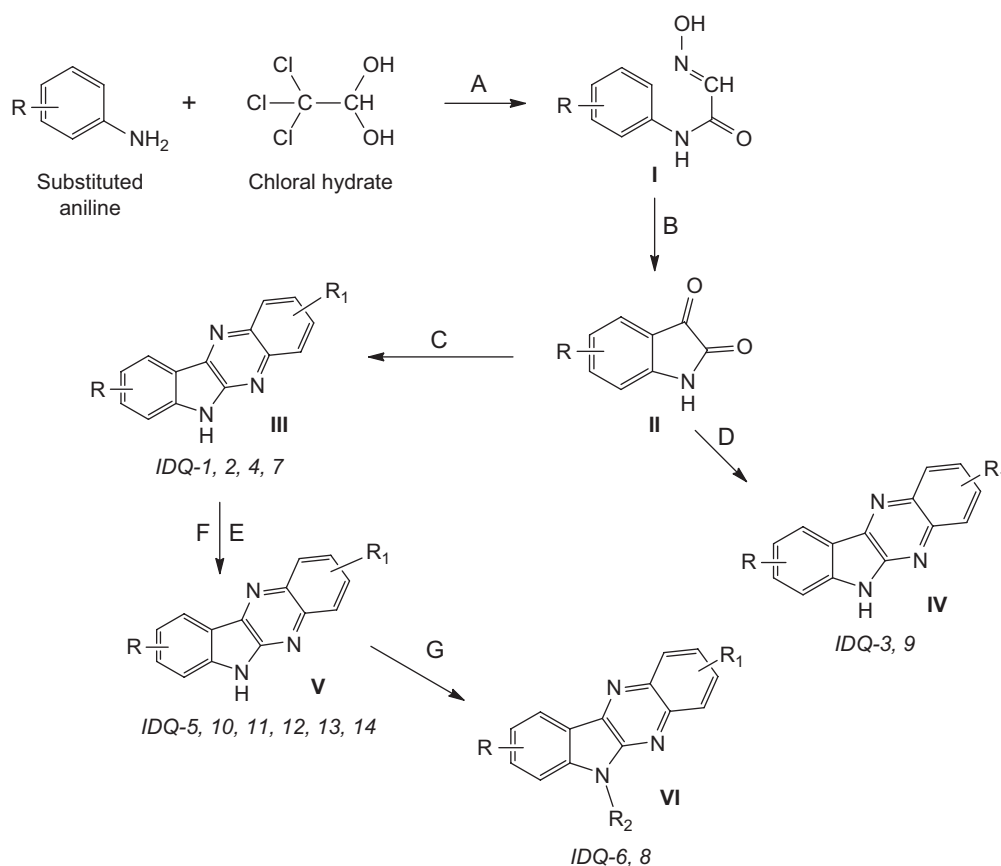
The 6*H*-indolo[2,3-*b*]quinoxaline derivatives were synthesized as illustrated in Scheme 1. Isatins, which served as key intermediates, were prepared from the appropriately substituted anilines using Sandmeyer methodology^{18,19}. Condensation of the synthesized isatins with the appropriate *o*-phenylenediamines in glacial acetic acid or hydrochloric acid and ethanol or formic acid at reflux temperature afforded 6*H*-indolo[2,3-*b*]quinoxaline derivatives (IDQ-1 to IDQ-4, IDQ-7, and IDQ-9) in good yields. The *N*-ethyl derivatives of 6*H*-indolo[2,3-*b*]quinoxalines (IDQ-6 and IDQ-8) were generated by ethyl iodide-potassium carbonate alkylation of compounds IDQ-1 and IDQ-7 at 85°C for 15 h.

6*H*-Indolo[2,3-*b*]quinoxaline-7-carboxamide (IDQ-5) was obtained from amide bond formation between an activated form of the corresponding acid (IDQ-2) and dimethyl amine. The synthesis of *N*-alkyl-6*H*-indolo[2,3-*b*]quinoxaline-9-amine (IDQ-10 to IDQ-14) was achieved by heating a reaction mixture containing 9-bromo-6*H*-indolo[2,3-*b*]quinoxaline (IDQ-7) and the appropriate secondary amine in dimethylformamide (DMF) at 120°C.

Experimental

Materials used

Reagents, starting materials, and solvents were purchased from common commercial suppliers (CDH, S.D. Fine, Loba, E. Merck, Lancaster, etc.). The melting points were determined in open capillary tubes on a Jindal melting point apparatus and are reported uncorrected. ¹H nuclear magnetic resonance (NMR) spectra were recorded on a Bruker Avance DRX-2000 (300 MHz, Fourier transform (FT) NMR) spectrometer in dimethylsulfoxide (DMSO) and CDCl₃, with tetramethylsilane (TMS) as internal standard. Fast atom bombardment (FAB) mass spectra were recorded on a Jeol SX 102/DA-6000 mass spectrometer/data system using argon/xenon (6 kV, 10 mA) as the FAB gas. The accelerating voltage was 10 kV and the spectra were recorded at room temperature. *m*-Nitrobenzyl alcohol (NBA) was used as the



Scheme 1. Synthesis of 6*H*-indolo[2,3-*b*]quinoxaline derivatives. A: Conc. HCl, sodium sulfate, hydroxylamine HCl, reflux for 15 min; B: PPA/H₂SO₄, 56°C for 6 h/120°C for 6 h; C, D: *o*-phenylenediamine or diaminobenzoic acid, acetic acid/HCOOH, reflux for 1-7 h; E: CDI, dry DMF, stir at room temperature for 4 h, DCM, MgSO₄; F: dry DMF, 120°C, 30 min-2 h; G: K₂CO₃, dry DME, 85-100°C for 12-16 h.

matrix. Infrared (IR) absorption spectra were recorded on a Jasco FT/IR – 470 Plus machine, using KBr by diffuse reflectance method. Ultraviolet (UV) absorption studies were done on a Shimadzu Pharmaspec-UV 1700 spectrophotometer to determine λ_{max} of the compounds. Elemental analysis (C, H, N) was done on a PerkinElmer CHN rapid analyzer. All the compounds gave satisfactory analysis within $\pm 0.4\%$ of the theoretical values. The purity and reaction progress were monitored by thin layer chromatography (TLC) using silica gel-G on a glass plate as the stationary phase and different polarities of solvents as the mobile phase. Visualization was accomplished with UV light and/or iodine vapor.

Synthesis of 6H-indolo[2,3-b]quinoxaline derivatives

The synthesis of the selected 6H-indolo[2,3-b]quinoxaline derivatives is outlined in Scheme 1.

Isatin

Isatin was synthesized as per the reported procedure^{18,19}.

Isatin-7-carboxylic acid

Isatin-7-carboxylic acid was synthesized as per the reported procedure^{18,19}.

Isatin-5-carboxylic acid

A solution of *p*-aminobenzoic acid (3.15 g), chloral hydrate (3.5 g), and hydroxylamine hydrochloride (2.86 g) in concentrated sulfuric acid (2.5 mL) and water (150 mL) was heated at 90°C for 30 min and then kept at 4°C for 16 h. The cream-colored isonitroso intermediate (29.8 g (64%)) was filtered off, washed with water, and dried. This compound (1.5 g) was added with stirring in portions over 30 min to concentrated sulfuric acid (7.5 g) maintained at 60–65°C. The mixture was then heated at 95°C for 1 h and poured onto ice (60 g). The resulting brown solid was filtered, dissolved in 1M NaOH solution, and filtered, and the filtrate was taken to pH 2 with concentrated HCl to give isatin-5-carboxylic acid. (65%, MP 274–275°C).

5-Bromo-isatin

This was synthesized as per the reported procedure^{18,19}.

6H-Indolo[2,3-b]quinoxaline (IDQ-1)

A solution of isatin (10 mmol) and *o*-phenylenediamine (30 mmol) in acetic acid (10 mL) was refluxed for 15 min and the precipitate obtained on cooling for 10 h. A pale reddish-yellow color precipitate was obtained. The product was filtered and washed with water. The crude product was extracted with chloroform and the obtained product was recrystallized from acetic acid. TLC was performed with methanol:chloroform (3:7).

¹H NMR (300 MHz, δ /ppm in DMSO- d_6): 4.9 (br, s, 1H, NH), 6.55–6.57 (d, $J = 5.5$ Hz, 1H, Ar-H), 6.75–6.77 (d, $J = 6.1$ Hz, 1H, Ar-H), 7.07–7.10 (d, $J = 9.2$ Hz, 1H, Ar-H), 7.32–7.34 (d, $J = 6.2$ Hz, 1H, Ar-H), 7.60–7.62 (d, $J = 6.2$ Hz, 2H, Ar-H), 7.71–7.73 (d, $J = 9.0$ Hz, 1H, Ar-H), 7.95 (d, $J = 5$ Hz, 1H, Ar-H); IR (KBr/cm⁻¹): 3452 (N-H, stretching), 3057 (C-H (Ar,

stretching)), 1531 (C=N, stretching); FAB-MS m/z [M]⁺: 219; Elemental Analysis: Calcd. (Found) (%) for C₁₄H₉N₃: C 76.70 (76.77), H 4.14 (4.26), N 19.17 (19.25).

6H-Indolo[2,3-b]quinoxaline-3-carboxylic acid (IDQ-2)

A solution of isatin (10 mmol) and diaminobenzoic acid (30 mmol) in acetic acid (10 mL) and ethanol (5 mL) was refluxed for 30 min and the precipitate obtained on cooling for 10 h. A reddish-yellow color precipitate was obtained. The product was filtered and washed with water. The crude product was extracted with chloroform and ethyl acetate and the obtained product was recrystallized from DMSO. TLC was monitored with acetic acid:methanol:chloroform (1:3:6).

¹H NMR (300 MHz, δ /ppm in CDCl₃): 6.25 (br, s, 1H, NH), 6.66–6.68 (d, $J = 5.5$ Hz, 1H, Ar-H), 6.79–6.81 (d, $J = 6.1$ Hz, 1H, Ar-H), 7.07–7.25 (m, 3H, Ar-H), 7.53–7.5 (d, $J = 9.0$ Hz, 1H, Ar-H), 7.72–7.73 (d, $J = 9.2$ Hz, 1H, Ar-H), 12.69 (br, s, 1H, COOH); IR (KBr/cm⁻¹): 3061 (C-H (Ar, stretching)), 1771 (C=O carboxylic, stretching), 1514 (C=N, stretching), 1427 (C-O-H carboxylic, stretching); FAB-MS m/z [M]⁺: 263; Elemental Analysis: Calcd. (Found) (%) for C₁₅H₉N₃O₂: C 68.44 (68.47), H 3.45 (3.46), N 15.96 (15.95).

6H-Indolo[2,3-b]quinoxaline-7-carboxylic acid (IDQ-3)

A solution of isatin-7-carboxylic acid (10 mmol) and *o*-phenylenediamine (30 mmol) in acetic acid (10 mL) and DMF (1 mL) was refluxed for 30 min and a pink-yellow color precipitate was obtained on cooling for 10 h. The product was filtered and washed with water. The obtained product was recrystallized from DMSO. TLC was monitored with acetic acid:methanol:chloroform (1:3:6).

¹H NMR (300 MHz, δ /ppm in CDCl₃): 5.6 (br, s, 1H, NH), 7.40–7.42 (d, $J = 5.4$ Hz, 1H, Ar-H), 7.53–7.55 (d, $J = 6.1$ Hz, 1H, Ar-H), 7.69–7.71 (d, $J = 5.5$ Hz, 1H, Ar-H), 8.09–8.11 (d, $J = 6.6$ Hz, 1H, Ar-H), 8.32–8.34 (d, $J = 6.0$ Hz, 1H, Ar-H), 8.48–8.50 (d, $J = 5.8$ Hz, 1H, Ar-H), 9.06 (s, 1H, Ar-H), 12.68 (br, s, 1H, COOH); IR (KBr/cm⁻¹): 3575 (N-H polynuclear, stretching), 3102 (C-H (Ar, stretching)), 1706 (C=O carboxylic, stretching), 1515 (C=N, stretching), 1464 (C-O-H carboxylic, stretching); FAB-MS m/z [M]⁺: 263; Elemental Analysis: Calcd. (Found) (%) for C₁₅H₉N₃O₂: C 68.44 (68.64), H 3.45 (3.25), N 15.96 (15.78).

6H-Indolo[2,3-b]quinoxaline-9-carboxylic acid (IDQ-4)

A solution of isatin-9-carboxylic acid (10 mmol) and *o*-phenylenediamine (30 mmol) in acetic acid (10 mL) and DMF (1 mL) was refluxed for 30 min and a pink-yellow color precipitate was obtained on cooling for 10 h. The product was filtered and washed with water. The obtained product was recrystallized from DMSO. TLC was monitored with acetic acid:methanol:chloroform (1:3:6).

¹H NMR (300 MHz, δ /ppm in DMSO- d_6): 5.7 (br, s, 1H, N-H), 7.17–7.19 (m, 3H, Ar-H), 7.38–7.40 (d, $J = 6.0$ Hz, 1H, Ar-H), 7.57–7.59 (d, $J = 6.3$ Hz, 1H, Ar-H), 7.93–7.94 (d, $J = 9.0$ Hz, 1H, Ar-H), 8.17–8.20 (d, $J = 9.3$ Hz, 1H, Ar-H), 8.25 (br, s, 1H, Ar-H); IR (KBr/cm⁻¹): 3060 (C-H (Ar, stretching)),

1774 (C=O carboxylic, stretching), 1524 (C=N, stretching), 1422 (C-O-H carboxylic, stretching); FAB-MS m/z [M]⁺: 263; Elemental Analysis: Calcd. (Found) (%) for C₁₅H₉N₃O₂: C 68.44 (68.30), H 3.45 (3.40), N 15.96 (15.95).

6*H*-Indolo[2,3-*b*]quinoxaline-3-carboxylic acid dimethylamide (IDQ-5)

A mixture of IDQ-2 (10 mmol) and CDI (*N,N*-carbonyl diimidazole) (130 mg) was stirred with dry DMF (8 mL) at room temperature for 48 h. To this mixture, dimethylamine (10 mmol) was added and stirred at room temperature for a further 30 min. The volatile components were then removed under vacuum and the residue was dissolved in dichloromethane (20 mL) and washed with water (2 × 20 mL) and dried over magnesium sulfate. The solvent was removed under vacuum to provide the crude product which was recrystallized with DMSO. TLC was developed with methanol:chloroform (4:6).

¹H NMR (300 MHz, δ/ppm in DMSO-*d*₆): 2.89 (s, 6H, CON(CH₃)₂), 6.15 (br, s, 1H, NH), 7.00–7.20 (m, 3H, Ar-H), 7.36–7.38 (d, *J* = 6.2 Hz, 1H, Ar-H), 7.58–7.60 (d, *J* = 6.0 Hz, 1H, Ar-H), 7.65–7.68 (d, *J* = 9.2 Hz, 1H, Ar-H), 7.93–7.96 (d, *J* = 9.0 Hz, 1H, Ar-H); IR (KBr/cm⁻¹): 3095 (C-H (Ar, stretching)), 2803 (C-H, stretching), 1692 (C=O amide, stretching), 1515 (C=N, stretching). FAB-MS m/z [M]⁺: 290; Elemental Analysis: Calcd. (Found) (%) for C₁₇H₁₄N₄O: C 70.33 (70.30), H 4.86 (4.80), N 19.30 (19.25).

6-Ethyl-indolo[2,3-*b*]quinoxaline (IDQ-6)

A mixture of 6*H*-indolo[2,3-*b*]quinoxaline (10 mmol), ethyl iodide (20 mmol), and potassium carbonate (22 mmol) in dry DMF (35 mL) was heated at 85°C for 12 h. After cooling, the precipitate formed was filtered, washed with water, and recrystallized in DMF. TLC was performed using methanol:chloroform (3:7)

¹H NMR (300 MHz, δ/ppm in DMSO-*d*₆): 1.24–1.28 (t, *J* = 6.9 Hz, 3H, CH₃), 3.11–3.23 (m, 2H, CH₂), 7.70–7.71 (m, 4H, Ar-H), 8.11–8.15 (dd, *J* = 1.5, 8.9 Hz, 2H, Ar-H), 8.24–8.27 (dd, *J* = 1.5, 8.6 Hz, 2H, Ar-H); IR (KBr/cm⁻¹): 3102 (C-H (Ar, stretching)), 2904 (C-H, stretching), 1547–1490 (C=N, stretching); FAB-MS m/z [M]⁺: 247; Elemental Analysis: Calcd. (Found) (%) for C₁₆H₁₃N₃: C 77.71 (77.78), H 5.30 (5.26), N 16.99 (16.97).

9-Bromo-6*H*-indolo[2,3-*b*]quinoxaline (IDQ-7)

A solution of 5-bromo-isatin (10 mmol) and *o*-phenylenediamine (30 mmol) in formic acid (10 mL) was refluxed for 15 min and a reddish-yellow color precipitate was obtained on cooling for 10 h. The product was filtered and washed with water. The crude product was dissolved in hot DMSO and filtered. TLC was monitored with methanol:chloroform (3:7).

¹H NMR (300 MHz, δ/ppm in DMSO-*d*₆): 5.7 (br, s, 1H, NH), 7.31 (s, 1H, Ar-H), 7.49–7.50 (d, *J* = 1.2 Hz, 1H, Ar-H), 7.59–7.60 (d, *J* = 1.2 Hz, 1H, Ar-H), 8.08–8.11 (dd, *J* = 1.2, 8.4 Hz, 2H, Ar-H), 8.24–8.28 (dd, *J* = 1.2, 8.4 Hz, 2H, Ar-H); IR (KBr/cm⁻¹): 3122 (C-H (Ar, stretching)), 1545 (C=N, stretching), 950 (C-Br, bending); FAB-MS m/z [M]⁺: 297; Elemental

Analysis: Calcd. (Found) (%) for C₁₄H₈N₃Br: C 56.40 (56.28), H 2.70 (2.76), N 14.09 (13.97).

6-Ethyl-9-bromo-indolo[2,3-*b*]quinoxaline (IDQ-8)

A mixture of 9-bromo-indolo[2,3-*b*]quinoxaline (10 mmol), ethyl iodide (20 mmol), and potassium carbonate (22 mmol) in dry DMF (35 mL) was heated at 85°C for 15 h. After cooling, the precipitate was filtered, washed with water, and recrystallized in DMF. TLC was run on methanol:chloroform (3:7).

¹H NMR (300 MHz, δ/ppm in DMSO-*d*₆): 1.23–1.27 (t, *J* = 6.9 Hz, 3H, CH₃), 3.24–3.43 (m, 2H, CH₂), 7.29 (s, 1H, Ar-H), 7.51–7.53 (d, *J* = 1.6 Hz, 1H, Ar-H), 7.62–7.64 (d, *J* = 1.6 Hz, 1H, Ar-H), 8.11–8.15 (dd, *J* = 1.6, 8.9 Hz, 2H, Ar-H), 8.28–8.32 (dd, *J* = 1.6, 8.9 Hz, 2H, Ar-H); IR (KBr/cm⁻¹): 3140 (C-H (Ar, stretching)), 2965 (C-H, stretching), 1567 (C=N, stretching), 990 (C-Br, bending); FAB-MS m/z [M]⁺: 326; Elemental Analysis: Calcd. (Found) (%) for C₁₆H₁₂N₃Br: C 58.91 (58.78), H 3.71 (3.66), N 12.88 (12.97).

9-Bromo-[6*H*-indolo[2,3-*b*]quinoxaline]-3-carboxylic acid (IDQ-9)

A solution of 5-bromo-isatin (10 mmol) and diaminobenzoic acid (30 mmol) in acetic acid (10 mL) and ethanol (5 mL) was refluxed for 30 min and a greenish-yellow color precipitate was obtained on cooling for 10 h. The crude product was filtered and washed with water and recrystallized in DMSO. TLC was monitored with acetic acid:methanol:chloroform (1:3:6).

¹H NMR (300 MHz, δ/ppm in DMSO-*d*₆): 6.02 (br, s, 1H, NH), 7.59 (s, 1H, Ar-H), 7.81–7.82 (d, *J* = 1.6 Hz, 1H, Ar-H), 7.84–7.85 (d, *J* = 1.8 Hz, 1H, Ar-H), 8.05–8.06 (d, *J* = 1.8 Hz, 1H, Ar-H), 8.08–8.09 (d, *J* = 1.5 Hz, 1H, Ar-H), 8.25 (s, 1H, Ar-H), 10.25 (s, 1H, COOH); IR (KBr/cm⁻¹): 3110 (C-H (Ar, stretching)), 1742 (C=O carboxylic, stretching), 1514 (C=N, stretching), 1462 (C-O-H carboxylic, stretching), 978 (C-Br, bending); FAB-MS m/z [M]⁺: 342; Elemental Analysis: Calcd. (Found) (%) for C₁₅H₈N₃O₂Br: C 52.66 (52.78), H 2.36 (2.36), N 12.28 (12.17).

N,N-Dimethyl-[6*H*-indolo[2,3-*b*]quinoxaline]-9-amine (IDQ-10)

A mixture of 9-bromo-6*H*-indolo[2,3-*b*]quinoxaline derivative (5.5 mmol) and dimethylamine (30 mmol) in dry DMF (5 mL) was heated at 120°C for 1 h. After cooling, the precipitate was filtered off and digested with hot ethyl acetate to give the product. The crude product was recrystallized with DMF/DMSO and TLC was monitored with methanol:chloroform (3:7).

¹H NMR (300 MHz, δ/ppm in DMSO-*d*₆): 2.51 (br, s, 6H, N(CH₃)₂), 5.90 (s, 1H, NH), 7.36 (s, 1H, Ar-H), 7.61–7.62 (d, *J* = 1.9 Hz, 1H, Ar-H), 7.72–7.73 (d, *J* = 1.5 Hz, 1H, Ar-H), 8.08–8.11 (dd, *J* = 1.2, 9.6 Hz, 2H, Ar-H), 8.24–8.27 (dd, *J* = 1.2, 9.6 Hz, 2H, Ar-H); IR (KBr/cm⁻¹): 3120 (C-H (Ar, stretching)), 2890 (C-H, stretching), 1535 (C=N, stretching), 1050 (C-N, bending); FAB-MS m/z [M]⁺: 262; Elemental Analysis: Calcd. (Found) (%) for C₁₆H₁₄N₄: C 73.26 (73.38), H 5.38 (5.16), N 21.36 (21.47).

N,N-Diethyl-[6H-indolo[2,3-b]quinoxaline]-9-amine (IDQ-11)

A mixture of 9-bromo-6*H*-indolo[2,3-*b*]quinoxaline derivative (5.5 mmol) and diethylamine (30 mmol) in dry DMF (5 mL) was heated at 120°C for 2–3 h. After cooling, the precipitate was filtered off and digested with hot ethyl acetate to give the product. The crude product was recrystallized with DMF/DMSO and TLC was monitored with methanol:chloroform (4:6).

¹H NMR (300 MHz, δ/ppm in DMSO-*d*₆): 1.2–1.26 (t, *J* = 6.9 Hz, 6H, (CH₃)₂), 3.20–3.34 (m, 4H, CH₂), 5.98 (br, s, 1H, NH), 6.48–6.51 (d, *J* = 1.5 Hz, 1H, Ar-H), 8.06–8.10 (dd, *J* = 1.5, 8.6 Hz, 2H, Ar-H), 8.11–8.15 (d, 2H, Ar-H), 8.25–8.29 (dd, *J* = 1.5, 8.6 Hz, 2H, Ar-H); IR (KBr/cm⁻¹): 3115 (C-H (Ar, stretching)), 2985 (C-H, stretching), 1535 (C=N, stretching); FAB-MS *m/z* [M + H]⁺: 290; Elemental Analysis: Calcd. (Found) (%) for C₁₈H₁₈N₄: C 74.46 (74.78), H 6.25 (6.16), N 19.30 (19.28).

4-(6H-Indolo[2,3-b]quinoxalin-9-yl)morpholine (IDQ-12)

A mixture of 9-bromo-6*H*-indolo[2,3-*b*]quinoxaline derivative (5.5 mmol) and *N*-morpholine (30 mmol) in dry DMF (5 mL) was heated at 120°C for 30 min–2 h. After cooling, the precipitate was filtered off and digested with hot ethyl acetate to give the product. The crude product was recrystallized with DMF/DMSO and TLC was monitored with methanol:chloroform (3:7).

¹H NMR (300 MHz, δ/ppm in DMSO-*d*₆): 2.69–2.75 (m, 4H, CH₂ morphonyl), 3.34–3.46 (m, 4H, CH₂, morphonyl), 6.03 (br, s, 1H, NH), 7.33–7.36 (d, *J* = 7.8 Hz, 1H, Ar-H), 7.60 (s, 1H, Ar-H), 7.73–7.75 (d, *J* = 6.9 Hz, 1H, Ar-H), 8.08–8.11 (dd, *J* = 1.2, 8.9 Hz, 2H, Ar-H), 8.25–8.28 (dd, *J* = 1.5, 8.9 Hz, 2H, Ar-H); IR (KBr/cm⁻¹): 3150 (C-H (Ar, stretching)), 2885 (C-H, stretching), 1572 (C=N, stretching), 1475 (C-O, stretching); FAB-MS *m/z* [M]⁺: 304; Elemental Analysis: Calcd. (Found) (%) for C₁₈H₁₆N₄O: C 71.04 (71.08), H 5.30 (5.26), N 18.41 (18.57).

9-(Piperidin-1-yl)-6H-indolo[2,3-b]quinoxaline (IDQ-13)

A mixture of 9-bromo-6*H*-indolo[2,3-*b*]quinoxaline derivative (5.5 mmol) and *N*-piperidine (30 mmol) in dry DMF (5 mL) was heated at 120°C for 5 h. After cooling, the precipitate was filtered off and digested with hot ethyl acetate to give the product. The crude product was recrystallized with DMF/DMSO and TLC was monitored with methanol:chloroform (3:7).

¹H NMR (300 MHz, δ/ppm in DMSO-*d*₆): 1.88–1.93 (m, 6H, CH₂, piperidinyl), 2.50–2.52 (m, 4H, CH₂, piperidinyl), 6.2 (br, s, 1H, NH), 7.59 (s, 1H, Ar-H), 7.78–7.79 (d, *J* = 1.2 Hz, 2H, Ar-H), 8.08–8.12 (dd, *J* = 1.2, 8.4 Hz, 2H, Ar-H), 8.25–8.28 (dd, *J* = 1.2, 8.4 Hz, 2H, Ar-H); IR (KBr/cm⁻¹): 3122 (C-H (Ar, stretching)), 1520 (C=N, stretching), 1038 (C-N, bending); FAB-MS *m/z* [M]⁺: 302; Elemental Analysis: Calcd. (Found) (%) for C₁₉H₁₈N₄: C 75.47 (75.78), H 6.00 (6.01), N 18.53 (18.57).

9-(4-Methylpiperizin-1-yl)-6H-indolo[2,3-b]quinoxaline (IDQ-14)

A mixture of 9-bromo-6*H*-indolo[2,3-*b*]quinoxaline derivative (5.5 mmol) and *N*-methyl piperazine (30 mmol) in dry DMF (5 mL) was heated at 120°C for 4–5 h. After cooling, the precipitate was filtered off and digested with hot ethyl acetate to give the product. The crude product was recrystallized with DMF/DMSO and TLC was monitored with methanol:chloroform (3:7).

¹H NMR (300 MHz, δ/ppm in DMSO-*d*₆): 2.46–2.52 (m, 4H, CH₂), 2.73 (s, 3H, CH₃), 3.29–3.36 (m, 4H, CH₂), 5.78 (br, s, 1H, NH), 7.30–7.31 (d, *J* = 1.5 Hz, 1H, Ar-H), 7.36 (s, 1H, Ar-H), 7.90–7.91 (d, *J* = 1.8 Hz, 1H, Ar-H), 8.08–8.11 (dd, *J* = 1.9, 9.0 Hz, 2H, Ar-H), 8.25–8.28 (dd, *J* = 1.9, 9.0 Hz, 2H, Ar-H); IR (KBr/cm⁻¹): 3132 (C-H (Ar, stretching)), 2885 (C-H, stretching), 1572 (C=N, stretching), 1475 (C-O, stretching); FAB-MS *m/z* [M]⁺: 317; Elemental Analysis: Calcd. (Found) (%) for C₁₉H₁₉N₅: C 71.90 (71.78), H 6.03 (6.06), N 22.07 (21.97).

***In vitro* cytotoxicity assay in human tumor cell lines**

The cytotoxicity of the synthesized compounds was screened in the HL-60 cell line by adopting the well-established MTT colorimetric microculture assay method^{20,21}.

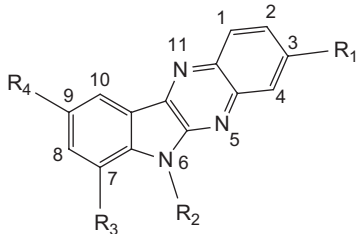
Increasing concentrations of each drug were placed with HL-60 tumor cell suspension (5 × 10⁴ cells/well). Cell growth was determined 72 h later by adding 50 μL of 3-(4,5-dimethylthiazol-2-yl)-2,5-diphenyltetrazolium bromide (MTT) (2.5 mg/mL). This was reduced by mitochondrial dehydrogenase of viable cells in an insoluble blue formazan product during the 4 h contact period at 37°C. After the supernatant was removed, the formazan crystals were solubilized by adding DMSO (100 μL). These plates were read at 550 nm with an enzyme linked immunosorbent assay (ELISA) reader. At each dose level of the compounds tested, cell growth inhibition was expressed as a fractional decrease of 550 nm absorbance in the treated cultures with respect to control and reference compounds (cisplatin and 5-fluorouracil) (Table 1).

***In silico* ADMET study**

A Pentium 4 workstation and Pallas 6.1.1 software were used to calculate and predict the ADMET (absorption, distribution, metabolism, excretion, toxicity) properties of the molecules^{22,23}. ChemDraw ultra software was used to draw the structures of the compounds to be analyzed, which were saved as an MDL file. The sketched molecules were subjected to calculation of the following properties: drug-likeness, metabolism, toxicity etc.

Quantitative structure–activity relationship analysis

The quantitative structure–activity relationship (QSAR) study of the synthesized compounds was carried out employing MOE and Dragon software^{24,25} running on a Pentium 4 computer. The compounds were sketched in ChemDraw software²⁶. The lowest energy conformers and physicochemical descriptors were calculated from MOE and Dragon software²⁷ (Table 2). The correlation between the activity and

Table 1. Structural variations and cytotoxicity of 6*H*-indolo[2,3-*b*]quinoxaline derivatives.


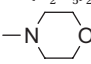
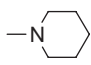
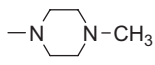
Compound code	R ₁	R ₂	R ₃	R ₄	Cytotoxicity (IC ₅₀ , μM)
IDQ-1	H	H	H	H	92
IDQ-2	-COOH	H	H	H	75
IDQ-3	H	H	-COOH	H	93
IDQ-4	H	H	H	-COOH	141
IDQ-5	-CON(CH ₃) ₂	H	H	H	27
IDQ-6	H	-C ₂ H ₅	H	H	38
IDQ-7	H	H	H	-Br	118
IDQ-8	H	-C ₂ H ₅	H	-Br	64
IDQ-9	-COOH	H	H	-Br	112
IDQ-10	H	H	H	-N(CH ₃) ₂	22
IDQ-11	H	H	H	-N(C ₂ H ₅) ₂	33
IDQ-12	H	H	H		58
IDQ-13	H	H	H		47
IDQ-14	H	H	H		38
Standard				Cisplatin	7
Standard				5-FU	266

Table 2. Molecular descriptors used for modeling cytotoxicity of 6*H*-indolo[2,3-*b*]quinoxaline derivatives.

-LogIC ₅₀	Mp	nCIC	RBF	nCp	nCOOHPh
4.0362	0.74	4	0	0	0
4.1249	0.73	4	0.03	0	1
4.0315	0.73	4	0.03	0	1
3.8508	0.73	4	0.03	0	1
4.5686	0.7	4	0.08	2	0
4.4202	0.71	4	0.06	1	0
3.9281	0.79	4	0	0	0
4.1938	0.75	4	0.06	1	0
3.9508	0.78	4	0.03	0	1
4.6576	0.7	4	0.08	2	0
4.4815	0.68	4	0.12	2	0
4.2366	0.69	5	0	0	0
4.3279	0.69	5	0	0	0
4.4202	0.68	5	0.02	1	0

the physicochemical descriptors was calculated using the partial least squares method.

The dataset comprises 14 6*H*-indolo[2,3-*b*]quinoxaline derivatives with cytotoxic activity against a human leukemia (HL-60) cell line. The cytotoxic activity of compounds in the series is reported as the IC₅₀ value, where IC₅₀ refers to the experimentally determined concentration required to inhibit 50% cell growth.

Statistical analysis was done by multiple linear regression using statistical software SYSTAT²⁸. QSAR models for

the series were constructed by stepwise variable selection, and best regressions were selected on the basis of the statistical quality. The quality of the regression models was judged from statistical parameters such as correlation coefficient *R* and squared correlation coefficient *R*², Fisher ratio value, *t*-statistic, and standard error of the estimate (SEE). Guidelines for the acceptance of regressions were: correlation coefficient, *R* = 0.90 or higher (variance, *R*² > 0.70); minimum intercorrelation between descriptors found in the same model (<0.6); Fisher ratio and *t*-statistic values indicating 95% level of significance.

The orthogonality of descriptors selected for formulating statistically significant correlations in multiple linear regression (MLR) calculations was established by generation of the correlation matrix and calculation of variance inflation factor (VIF) values. The VIF value was calculated from 1/1 - *R*², where *R*² is the multiple correlation coefficient of one descriptor's effect regressed on the remaining molecular descriptors. VIF values larger than 5 indicate that the information of the descriptors may be hidden by the correlation of the descriptors.

Validation of the selected correlations was performed using the in-house program VALSTAT²⁹. The reliability of the QSAR correlations was tested in a cross-validation method with determination of cross-validated *R*² or *Q*². Values of *Q*² can be considered as proof of high predictive ability of the QSAR model. Further confirmation of the predictive power of the generated models was obtained by calculation of the standard deviation based on the predicted residual sum of

Table 3. Physicochemical characteristic of 6*H*-indolo[2,3-*b*]quinoxaline derivatives.

Compound code	Molecular formula	Molecular weight		Melting point ^b	Solubility	Rf value	λ_{\max}	Yield
		Calcd.	Found ^a					
IDQ-1	C ₁₄ H ₉ N ₃	219.24	219	215–218°C	Methanol	0.89	306, 356	85%
IDQ-2	C ₁₅ H ₉ N ₃ O ₂	263.25	263	180–182°C	DMSO, methanol	0.82	395.5, 280	77%
IDQ-3	C ₁₅ H ₉ N ₃ O ₂	263.25	263	320–323°C	DMSO, methanol	0.20	356, 281	65%
IDQ-4	C ₁₅ H ₉ N ₃ O ₂	263.25	263	170–172°C	Methanol	0.60	333.5	62%
IDQ-5	C ₁₇ H ₁₄ N ₄ O	290.32	290	217–220°C	DMSO, methanol	0.42	265.5, 370	56%
IDQ-6	C ₁₆ H ₁₃ N ₃	247.29	247	248–251°C	DMSO	0.75	346.5, 394.5	72%
IDQ-7	C ₁₄ H ₈ BrN ₃	298.14	297	275–277°C	DMF, acetone	0.92	356	90%
IDQ-8	C ₁₆ H ₁₂ BrN ₃	326.19	326	229–230°C	DMF, acetone	0.44	355.5, 265.5	64%
IDQ-9	C ₁₅ H ₈ BrN ₃ O ₂	342.15	342	320–323°C	DMSO, DMF	0.56	355.5, 265.5	60%
IDQ-10	C ₁₆ H ₁₄ N ₄	262.31	262	280–282°C	DMF, acetone	0.80	280, 357	75%
IDQ-11	C ₁₈ H ₁₈ N ₄	290.36	290	310–312°C	DMSO, acetone	0.48	355, 306.5, 263	80%
IDQ-12	C ₁₈ H ₁₆ N ₄ O	304.35	304	350–352°C	DMF, acetone	0.51	268, 329	70%
IDQ-13	C ₁₉ H ₁₈ N ₄	302.37	302	326–330°C	DMSO, DMF	0.51	279, 354	72%
IDQ-14	C ₁₉ H ₁₉ N ₅	317.39	317	>360°C	DMF, acetone	0.63	281, 355	67%

^aMW found by mass spectrometry.

^bMP, open capillary method, uncorrected.

squares (S_{PRESS}) and standard deviation of error of prediction (SDEP) values.

Results and discussion

The series of 6*H*-indolo[2,3-*b*]quinoxaline derivatives was synthesized as per Scheme 1, and their physicochemical properties were calculated and are given in Table 3. The structures of the synthesized compounds were confirmed as follows. The FAB mass spectra of the synthesized compounds showed molecular weights which corresponded to molecular weights calculated from the respective molecular formulae. Further, the results of elemental analysis of the compounds showed that the experimental values coincided with the calculated values and errors lay within $\pm 0.4\%$ of the calculated values. ^1H NMR spectra were used to determine the number and environment of hydrogen atoms.

Cytotoxic activity

The IC_{50} values of the synthesized 6*H*-indolo[2,3-*b*]quinoxaline derivatives were determined against the HL-60 cancer cell line employing the MTT assay in 96-well plates (Table 1). Cisplatin and 5-fluorouracil were used as reference compounds. Except for three compounds (IDQ-4, IDQ-7, and IDQ-9), all compounds were cytotoxic at micromolar concentrations. Compounds IDQ-5, IDQ-6, IDQ-10, IDQ-11, and IDQ-14 were found to be the most active in the present series. The nature of the substituent in ring A of 6*H*-indolo[2,3-*b*]quinoxaline appears to play a significant role in the cytotoxicity exhibited by these analogs. The presence of a free carboxylic group in the 6*H*-indolo[2,3-*b*]quinoxaline nucleus, with the exception of compound IDQ-2, irrespective of its position, decreases the cytotoxic potency to a major extent. However, the 6*H*-indolo[2,3-*b*]quinoxaline derivative with a carboxyl moiety on C-7 (IDQ-2) showed a marginal increase in cytotoxic potency. Conversion of the carboxylic group in IDQ-2 to the dimethyl carboxamido moiety (IDQ-5) caused a significant increase in cytotoxic

activity. This marked increase in cytotoxic potency might be due to the compound's structural similarity to acridine-4-carboxamide. Another important finding is that the *N*-ethyl derivatives of 6*H*-indolo[2,3-*b*]quinoxaline are more cytotoxic than their unsubstituted analogs. Bromo substitution at the C-9 atom of the 6*H*-indolo[2,3-*b*]quinoxaline decreases the cytotoxic activity, whereas replacing the bromo group with a secondary amino group improves the cytotoxicity; compound IDQ-10 with a dimethylamino group at the C-9 atom of 6*H*-indolo[2,3-*b*]quinoxaline was the most potent. Furthermore, increasing the carbon chain length or cyclicity of the alkyl group on the nitrogen atom reduces the cytotoxic potency.

In silico ADMET study

Clinical failure of most intercalator cytotoxic drugs is mainly due to their pharmacokinetic attributes rather than to pharmacodynamics. Hence, optimizing the pharmacokinetic properties during the stages of drug development is now widely accepted as being essential. With the abovementioned view, ADME attributes of the designed compounds were determined computationally prior to their synthesis. Moreover, solubility, pKa, and lipophilicity are integrally linked with chemical structure³⁰.

In order to validate the proposed compounds on the guidelines of the Lipinski "rule of 5" (molecular weight >500, logP >5, hydrogen bond donors (HBD) >5, and hydrogen bond acceptors (HBA) >10), an *in silico* ADMET study on the proposed compounds was carried out using Pallas 3.1.1.2 software. The relevance of the designed molecules with respect to the Lipinski rule of 5 is as follows^{10,31}.

The molecular weight of the proposed compounds lies in the range 219.24–342.15, which is well within the limits prescribed by the Lipinski rule of 5. LogP is a crucial factor governing passive membrane partitioning and thereby influencing permeability. In light of this dependence, it has been suggested that absorption may be optimal within a logP range of 1–4. The logP value of most of the synthesized

compounds lies between 1 and 4, with the exception of compound IDQ-8 ($\log P = 4.35$). The optimum range of the calculated $\log P$ values of the proposed compounds shows that the compounds are most suitable for passive transcellular

absorption across intestinal epithelia. Compound IDQ-8 possess $\log P > 4$, so it is highly likely that the compound can undergo renal reabsorption and will have a prolonged half-life ($t_{1/2}$) value due to its high lipophilicity.

Table 4. Lipinski parameters of the compounds.

Compound code	MW	LogP	HBD	HBA
IDQ-1	219.26	2.95	1	2
IDQ-2	263.27	2.53	1	4
IDQ-3	263.27	2.53	1	4
IDQ-4	263.27	2.53	1	4
IDQ-5	290.35	2.28	1	3
IDQ-6	247.32	3.59	0	2
IDQ-7	298.15	3.71	1	2
IDQ-8	326.21	4.35	0	2
IDQ-9	342.16	3.29	1	4
IDQ-10	262.34	3.01	1	2
IDQ-11	290.40	3.90	1	2
IDQ-12	304.38	2.23	1	3
IDQ-13	302.41	3.96	1	2
IDQ-14	317.43	2.13	1	2
Cisplatin	247.2	0.00	2	0
5-fluorouracil	130.09	-0.69	2	2

Note. MW, molecular weight; HBD, hydrogen bond donor; HBA, hydrogen bond acceptor.

Atoms of both HBD type and HBA type are molecular determinants responsible for binding affinity and specificity, e.g. hydrogen bonds. Hydrogen bond acceptor and donor groups in the compound optimize the drug-receptor interaction. The number of hydrogen atoms, i.e. ≤ 10 hydrogen bond acceptors and ≤ 5 hydrogen bond donors in the proposed compounds, obeys the Lipinski rule of 5. Thus the proposed molecules may have good absorption or permeability properties through the biological membrane in addition to enhanced binding affinity and specificity toward the receptor.

The predicted drug-likeness index highlights whether or not the proposed compounds follow the Lipinski rule of 5. It is quite evident from the results recorded in Table 4 that the Lipinski parameters calculated for the proposed compounds are in the ranges recommended by the Lipinski rule of 5, though adherence to the aforementioned rule is not an essential requirement for anticancer compounds.

The ionization state of a compound *in vivo* can be predicted by considering its pK_a relative to pH in various body compartments. pK_a is the primary determinant of the solubility of a compound. *In vivo*, this has a decisive

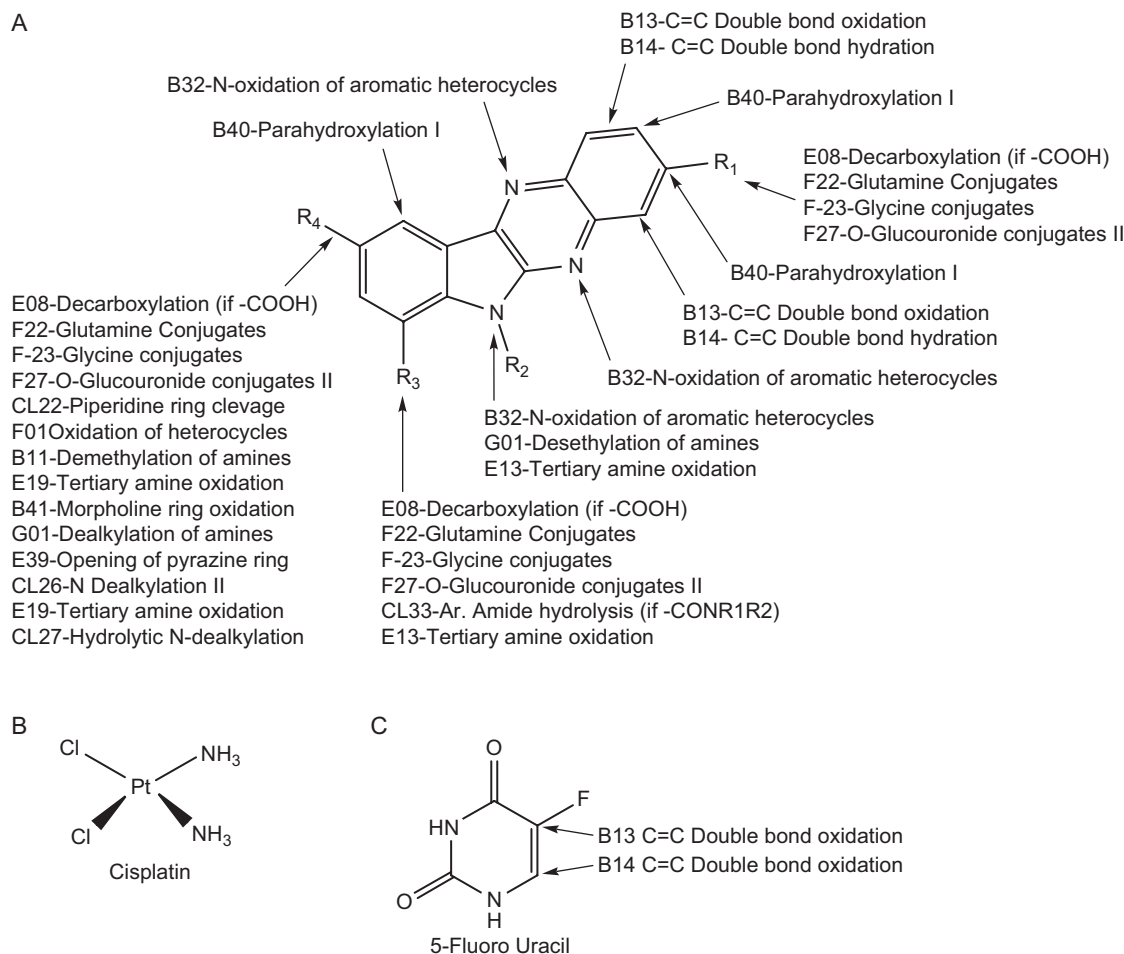


Figure 1. Position of the metabolites of 6H-indolo[2,3-b]quinoxaline derivatives (A), cisplatin (B), and 5-fluorouracil (C).

bearing on oral absorption, following the premise that drugs must dissolve in the gastrointestinal (GI) tract to cross the intestinal membrane. The proposed compounds have optimum pKa (3.29–11.91), which suggests that they may be absorbed orally and undergo proper distribution between compartments^{31,32}.

The formation of reactive metabolic intermediates is one of the causes of drug toxicity. Oxidation to electrophilic intermediates or reduction to nucleophilic radicals that can attach DNA or RNA and induce carcinogenicity are two major reactions by which toxicity is exerted. Although many leads are abandoned early on in the drug discovery stage due to a toxic metabolite, this does not always imply toxicity in a given drug candidate, since there are other factors that can make the metabolite toxic or non-toxic. The presence of a toxic metabolite, however, raises a red flag, which must be extensively examined in animal toxicity studies³³.

Metabolites of the proposed compounds were predicted employing the MetaboloExpert module of Pallas software (Figure 1). The 6*H*-indolo[2,3-*b*]quinoxaline derivatives IDQ-2 to IDQ-4 were also predicted to form conjugates of glutamine, glycine, and glucouronide types of secondary metabolites, whereas another carboxylic derivative IDQ-9 was predicted to form only *o*-glucouronide and glutamine conjugated products. None of the proposed compounds was predicted to form methylated or acetylated products, which are toxic in nature.

The predicted toxicity studies indicated that the proposed compounds were free from neurotoxicity, immunotoxicity, and irritation. The 6*H*-indolo[2,3-*b*]quinoxaline compounds were devoid of significant teratogenicity. It is also noteworthy that the compounds predicted to form conjugated products are less likely to exhibit teratogenic toxicity (<17%). Furthermore, all the proposed compounds were predicted to have less (or no) teratogenic toxicity than the reference compound (5-fluorouracil (34%)).

Literature findings revealed that oxidation of aromatic rings can be prevented by substituting them with stronger electron withdrawing groups. With this rationale, the proposed compounds were designed to have electron withdrawing groups (NO₂, COOH, etc.) in the nucleus, which prevents oxidation of the aromatic ring. Furthermore, these groups also have the ability to interact with the receptor (DNA) through hydrogen bonding, which might help to stabilize the intercalated drug–DNA complex.

QSAR studies

Multiple linear regression treatment of the molecular descriptors (Table 2) calculated for 6*H*-indolo[2,3-*b*]quinoxaline derivatives and their corresponding activity parameters led to the development of several QSARs. The generated QSARs were thoroughly scrutinized for statistical validity and predictive potential as per the criteria described in the experimental section.

The best QSAR models derived for modeling the cytotoxic activity of 6*H*-indolo[2,3-*b*]quinoxaline derivatives are as follows.

Model 1

$$-\log IC_{50} = [3.059 (\pm 0.633)] + [0.281 (\pm 0.074)] nCp + [0.235 (\pm 0.147)] nCIC$$

$$n = 14, R = 0.93, R^2 = 0.87, \text{std} = 0.09, F = 37.4, Q^2 = 0.79, S_{\text{PRESS}} = 0.12, \text{SDEP} = 0.11$$

Model 2

$$-\log IC_{50} = [6.658 (\pm 1.748)] + [-3.433 (\pm 2.408)] Mp + [2.783 (\pm 2.135)] RBF + [-0.203 (\pm 0.171)] nCOOHPh$$

$$n = 14, R = 0.91, R^2 = 0.84, \text{std} = 0.11, F = 17.0, Q^2 = 0.65, S_{\text{PRESS}} = 0.172, \text{SDEP} = 0.146$$

In the QSAR models given above, *n* is the number of data points, *R* is the correlation coefficient, *R*² is the squared correlation coefficient, and *F* represents the Fisher ratio between the variances of calculated and observed activities (Table 5). The figures given in parentheses with ± sign in the model are 95% confidence limits.

The statistical relevance of models 1 and 2 is indicated as follows. The correlation coefficient values, *R*, show that they account for more than 90% of the variance in biological activity. The standard error of estimate is very low, demonstrating the accuracy of fit. The Fisher ratio values obtained for the QSARs exceed the tabulated value (8.51 for model 1 and 7.23 for model 2) by a large margin, as desired for a meaningful correlation. The coefficients are all significantly above the 95% level as established by their corresponding *t*-test values, given in Table 6. Furthermore, the calculated correlation matrix (Table 7) and VIF values (Table 6) indicate that the descriptors are not interrelated.

The above models (1 and 2) were validated using the leave-one-out (LOO) approach. The results of LOO cross-validations are given in Table 5. Plots of cross-validated activity values versus the experimental activity values of compounds in the training set using models 1 and 2 are shown in Figures 2–5, respectively. Based on the cross-validated results, it is evident that the models exhibit good predictive capacity. Further confirmation of the predictive

Table 5. Correlation matrix for descriptors in QSAR models of series I.

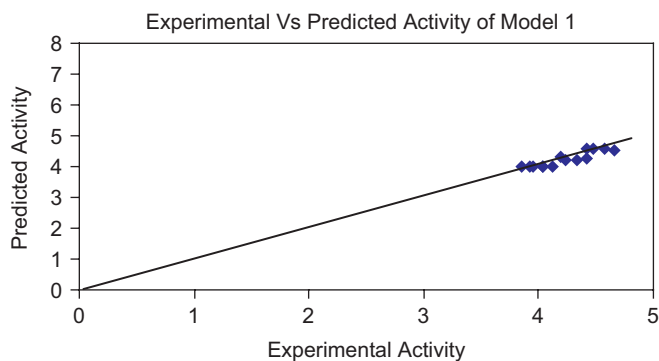
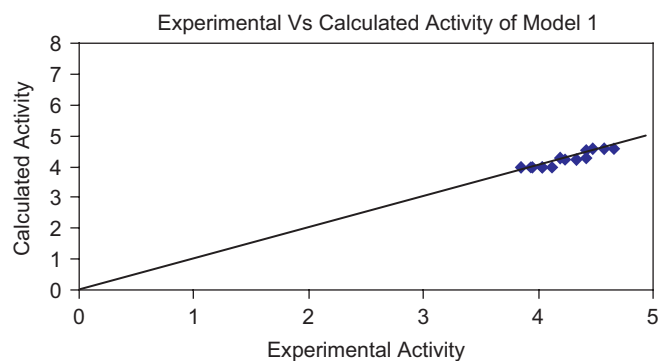
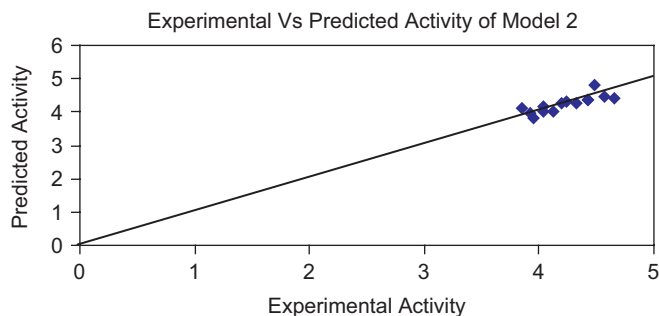
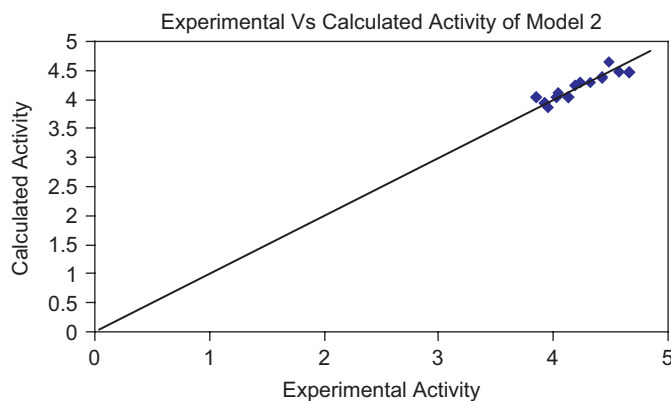
	–LogIC ₅₀	Mp	nCIC	RBF	nCp	nCOOHPh
–LogIC ₅₀	1.000	–0.755	0.208	0.618	0.851	–0.621
Mp		1.000	–0.537	0.339	–0.503	0.395
nCIC			1.000	–0.470	–0.199	–0.330
RBF				1.000	0.877	–0.153
nCp					1.000	–0.501
nCOOHPh						1.000

Table 6. Variance inflation factor (VIF) and *t*-values of descriptors in the QSAR models derived for series I.

Model	Effect	VIF	<i>t</i> -Value
Model 1	Constant	—	10.768
	nCP	1.041	8.438
	nCIC	1.041	3.566
Model 2	Constant	—	8.614
	Mp	1.307	–3.225
	RBF	1.129	2.949
	nCOOHPh	1.184	–2.677

Table 7. Experimental and predicted activity values of 6*H*-indolo [2,3-*b*]quinoxaline derivatives.

Experimental result	Model 1		Model 2	
	Predicted activity	Calculated activity	Predicted activity	Calculated activity
4.0362	3.99286	3.99939	4.14079	4.1175
4.1249	3.97713	3.99939	3.99945	4.03241
4.0315	3.9937	3.99939	4.03274	4.03241
3.8508	4.02576	3.99939	4.09715	4.03241
4.5686	4.55959	4.56206	4.45679	4.47745
4.4202	4.26535	4.28073	4.38303	4.38746
3.9281	4.01204	3.99939	3.96796	3.94584
4.1938	4.29031	4.28073	4.27018	4.25013
3.9508	4.00802	3.99939	3.80898	3.86076
4.6576	4.52601	4.56206	4.43662	4.47745
4.4815	4.59246	4.56206	4.81092	4.65742
4.2366	4.23332	4.23446	4.31165	4.28916
4.3279	4.18504	4.23446	4.27258	4.28916
4.4202	4.57527	4.51579	4.36528	4.37914

**Figure 2.** Graph showing correlation between experimental activity and predicted activity of model 1.**Figure 3.** Graph showing correlation between experimental activity and calculated activity of model 1.**Figure 4.** Graph showing correlation between experimental activity and predicted activity of model 2.**Figure 5.** Graph showing correlation between experimental activity and calculated activity of model 2.

ability was obtained from the PRESS statistics of the QSARs, the uncertainty in the prediction (S_{PRESS}) and standard error due to prediction (SDEP), which was less than 0.4.

Model 1 was found to be the most important biparametric correlation for modeling the cytotoxic activity of 6*H*-indolo[2,3-*b*]quinoxaline derivatives. The molecular descriptors incorporated into the model in stepwise regression analysis are the functional group count descriptor

nCp and constitutional descriptor nCIC. The descriptor nCp encodes information regarding the number of primary carbon atoms in the molecule; therefore, the positive coefficient associated with this term implies that an increase in the number of primary carbon atoms will cause a corresponding increase in the cytotoxic potency of 6*H*-indolo[2,3-*b*]quinoxaline derivatives. The second descriptor nCIC represents the number of rings in the molecule;

thus, the positive coefficient of this descriptor in model 1 suggests that the good cytotoxic activity of 6*H*-indolo[2,3-*b*]quinoxaline derivatives can be increased by incorporating substituents with rings.

As no further biparametric correlations of statistical significance could be obtained for the dataset, the study was extended for triparametric correlations, as they are permitted for a dataset of 14 compounds in accordance with the lower limit of rule of thumb³⁴. Model 2 was found to be the most important triparametric correlation obtained in the stepwise multiple linear regression analysis. The model comprises the following descriptor terms: mean atomic polarizability (Mp), rotatable bond fraction (RBF), and functional group count descriptors (nCOOHPh). The descriptor Mp represents the polarizable components in the molecule. The negative slope of the descriptor in the model implies that the presence of polarizable substituents in the molecule is not conducive for cytotoxic activity. The second descriptor, RBF, in model 2 encodes information about the flexibility of the substituents in the molecule. The positive coefficient of the parameter indicates that an increase in flexibility of the molecules will cause a corresponding increase in their cytotoxic potency. The last descriptor in model 2 is nCOOHPh, which represents the aromatic carboxylic groups in the molecule. The negative sign associated with the coefficient of this descriptor suggests that the presence of carboxylic functional groups on the tetracyclic ring is not conducive for cytotoxic activity of the 6*H*-indolo[2,3-*b*]quinoxaline derivatives.

From the discussion above, it is quite evident that presence of polar substituents is highly disfavored for cytotoxic activity of 6*H*-indolo[2,3-*b*]quinoxaline derivatives, whereas the presence of hydrophobic moieties (as accounted for by the descriptors nCp and nCIC in model 1) appears to have a positive effect on the same. To be specific, the cytotoxic activity of the 6*H*-indolo[2,3-*b*]quinoxalines is profoundly influenced by the alkyl substituents in the R2 position and the tertiary amino moiety in the R4 position of the tetracyclic ring. However, the positive effect of molecular flexibility cannot be reasoned, but it is probably due to the fact that the dimethyl and diethylamino substituents at R4 exhibit better potency than the cyclic counterparts such as piperidino, morpholino, and piperazino groups. Finally, it may be concluded that the mechanism of cytotoxic activity exhibited by 6*H*-indolo[2,3-*b*]quinoxaline is nonspecific in nature, as indicated by the findings of the QSAR study. Though the DNA intercalating ability of 6*H*-indolo[2,3-*b*]quinoxalines is well defined in the literature, the cytotoxic activity of synthesized 6*H*-indolo[2,3-*b*]quinoxalines appears to be dependent on the ability to cross the cell membrane and establish an optimum intracellular concentration.

Conclusion

In the present study, the rationale for designing a series of novel cytotoxic agents bearing structural resemblance to anticancer acridines has been presented. *In silico* pharmacokinetic studies were also performed in order to validate

the relevance of the proposed molecules on the basis of ADME and toxicity studies. Compounds with the desired pharmacokinetic profile were synthesized and structurally characterized. The novel 6*H*-indolo[2,3-*b*]quinoxaline derivatives exhibited significant activity *in vitro* against a human leukemia (HL-60) cell line. The data presented herein not only provide structural and mechanistic insight into newly synthesized compounds, but also provide new directions for the design of novel compounds, which will aid in the generation of more effective cytotoxic agents. In addition to this, QSAR studies were also performed on three series of compounds possessing cytotoxic activity in order to develop a set of guidelines for future design of potent analogs of the studied congeners that can be tailor-made to have enhanced anticancer activity. The results of the QSAR study presented here also lay the foundation for understanding the mechanism through which the molecules exert cytotoxic activity.

Acknowledgements

The authors are thankful to the Vice Chancellor, RGPV, Bhopal for providing laboratory facilities. Another of the authors (C.K.) would like to thank CSIR, New Delhi for providing a Senior Research Fellowship. The authors are also acknowledge CDRI, Lucknow and CNCI, Kolkata for their help in this work.

Declaration of interest: One of the authors (N.S.H.N.M.) would like to give his sincere thanks to AICTE, New Delhi for a grant from Career Award to Young Teachers.

References

1. http://www.pathology2.jhu.edu/bladder_cancer/glossary.cfm.
2. Jackson BG. Mechanism-based target identification and drug discovery in cancer research. *Science* 2000;287:1969-73.
3. American Cancer Society, Inc., Surveillance Research. Cancer Faiths and Figures, 2005. <http://www.geocities.com>.
4. World Health Organization. Cancer. February 2006. www.who.int/cancer/en. Retrieved on 25-06-2007.
5. Cancer Research UK. UK cancer incidence statistics by age. January 2007. www.cancerresearchuk.org. Retrieved on 25-06-2007.
6. Luc P, Stefaan VD, Mei G, Ruoli B, Ernest H, Arnold V, et al. Synthesis and biological evaluation of dihydrobenzofuran lignans and related compounds as potential antitumor agents that inhibit tubulin polymerization. *J Med Chem* 1999;42:5475-81.
7. Monish J, Chul-Hoon K. 1,2-Benzisoxazole phosphorodiamidates as novel anticancer prodrugs requiring bioreductive activation. *J Med Chem* 2003;46:5428-36.
8. Congiu C, Cocco MT, Lilliu V, Onnis V. New potential anticancer agents based on the anthranilic acid scaffold. Synthesis and evaluation of biological activity. *J Med Chem* 2005;48:8245-52.
9. http://jjco.oupjournals.org/cgi/content/full/32/suppl_1/S13.
10. Oprea TI. Virtual screening in lead discovery: a viewpoint. *Molecules* 2002;7:51-62.
11. Leslie WD, Antony JK, Graeme JF, Bruce CB, William AD. Positioning of the carboxamide side chain in 11-oxo-11*H*-indeno[1,2-*b*]quinolinecarboxamide anticancer agents: effects on cytotoxicity. *Bioorg Med Chem* 2001;9:445-52.
12. Martin YC, Kutter E, Austel V. The Medicinal Chemist's Approach, in *Modern Drug Research: Path to Better and Safer Drugs*. New York: Marcel Dekker, 1989:243-307.
13. Katrin MD, Stefanie L, Martin H, Manuela H, Kristian W, Michael L, et al. Synthesis of 6*H*-indolo[2,3-*b*]quinoxaline-*N*-glycosides and their

- cytotoxic activity against human ceratinocytes (HaCaT). *Org Biomol Chem* 2008;6:4218-23.
14. Wilhelmsson LM, Ngarita K, Jan B. Interactions of antiviral indolo[2,3-b]quinoxaline derivatives with DNA. *J Med Chem* 2008;51:7744-50.
 15. Harmenberg J, Wahren B, Bergman J, Akerfeldt S, Lundblad L. Antiherpesvirus activity and mechanism of action of indolo-(2,3-b)quinoxaline and analogs. *Antimicrob Agents Chemother* 1988;32:1720-4.
 16. Harmenberg J, Akesson JA, Graslund A, Malmfors T, Bergman J, Wahren B, et al. The mechanism of action of the anti-herpes virus compound 2,3-dimethyl-6(2-dimethylaminoethyl)-6H-indolo-(2,3-b)quinoxaline. *AntiViral Res* 1991;15:193-204.
 17. Paola BA, Brigitte B, William L, Christine B, France-Aimée A, Sylvain R, et al. DNA interaction and cytotoxicity of a new series of indolo[2,3-b]quinoxaline and pyridopyrazino[2,3-b]indole derivatives. *Chem Biol Interact* 2001;138:59-75.
 18. Silva JFM, Garden SJ, Pinto AC. The chemistry of isatins: a review from 1975 to 1999. *J Braz Chem Soc* 2001;12:273-324.
 19. Yen VQ, Buu-Hoi NP, Xuong ND. Fluorinated isatins and some of their heterocyclic derivatives. *J Org Chem* 1958;23:1858-61.
 20. Skehan P, Storeng R, Scudiero D, Monks A, McMahon J, Vistica D, et al. New colorimetric cytotoxicity assay for anticancer-drug screening. *J Natl Cancer Inst* 1990;82:1107-12.
 21. Mosmann T. Rapid colorimetric assay for cellular growth and survival: application to proliferation and cytotoxicity assays. *J Immunol Methods* 1983;65:55-63.
 22. Palas 3.1.1.2, ADME-Tox software. Sedona, AZ: CompuDrug International Inc., 2000.
 23. Moorthy NSHN, Rahul S, Hemendra PS, Gupta SD. Synthesis, biological evaluation and *in silico* metabolic prediction of flavanone derivatives. *Chem Pharm Bull* 2006;54:1384-90.
 24. MOE molecular modeling package. Montreal: Chemical Computing Group Inc., 2002.
 25. Dragon web version 3.0. Milano Chemometrics and QSAR Research Group, 2003. www.disat.uinmib.it.
 26. ChemOffice 2001. Bethesda, MD: Adept Scientific, CambridgeSoft Corp, UK, 2001.
 27. Lin A. QuaSAR-descriptors. *J Chem Comput Group*. http://www.chemcomp.com/Journal_of_CCG/Features/descr.htm.
 28. SYSTAT 10.2. Chicago, IL: Systat Software Inc., 2003.
 29. Gupta AK. VALSTAT. Indore, India: SGSITS, 2004.
 30. Beresford AP, Segall M, Tarbit MH. *In silico* prediction of ADME properties: are we making progress? *Curr Opin Drug Discov Dev* 2004;7:36-42.
 31. Hashida M. *In silico* prediction of pharmacokinetic properties. *Yakugaku Zasshi* 2005;125:853-61.
 32. McGee P. New *in vitro*, modeling tools may cut tox attrition. *Drug Discov Dev* 2005;8:55-60.
 33. White RE. High-throughput screening in drug metabolism and pharmacokinetic support of drug discovery. *Annu Rev Pharmacol Toxicol* 2000;40:133-57.
 34. Balaji S, Karthikeyan C, Hari Narayana Moorthy NS, Trivedi P. QSAR modeling of HIV-1 reverse transcriptase inhibition by benzoxazinones using a combination of P_VSA and pharmacophore feature descriptors. *Bioorg Med Chem Lett* 2004;14:6089-94.